9 Superconductivity and Magnetism

D.G. Eshchenko, H. Keller, R. Khasanov, S. Kohout (till August 2005), I. Landau (October till December 2005), F. La Mattina, A. Maisuradze, T. Paraiso (June 2005 till February 2006), J. Roos, A. Shengelaya (till November 2005), S. Strässle, S. Weyeneth (since October 2005)

Visiting scientists: A. Dooglav, V.A. Ivanshin, B. Kochelaev, I.M. Savić

Emeritus members: Prof. K.A. Müller (Honorarprofessor), Prof. T. Schneider (Titularprofessor), Dr. M. Mali

in collaboration with:
ETH Zürich (K. Conder, J. Karpinski), Paul Scherrer Institute (K. Conder, E. Morenzoni), Max-Planck-Institute for Solid State Research Stuttgart (A. Bussmann-Holder), IBM Rüschlikon Research Laboratory (J.G. Bednorz), University of Birmingham (E.M. Forgan), University of Rome (A. Bianconi, D. Di Castro), Kazan State University (A. Dooglav, M.V. Eremin, V. Ivanshin, B.I. Kochelaev), University of Belgrade (I.M. Savić), University of Tokyo (T. Sasagawa, H. Takagi)

In the last year we continued our research projects on the magnetic and electronic properties of novel superconductors and related materials by means of a combination of various complementary experimental techniques, such as muon-spin rotation (μSR), low-energy μSR (LE-μSR), electron paramagnetic resonance (EPR), nuclear magnetic resonance (NMR), nuclear quadrupole resonance (NQR), as well as SQUID and torque magnetometry. In particular, detailed isotope-effect and pressure-effect studies in novel superconductors were performed. The aim of our research activities is to explore the *macroscopic* and *microscopic* physical properties of cuprate high-temperature superconductors (HTS), other novel superconductors, and related materials in order to understand the basic physics of these systems. In addition, in collaboration with the IBM Rüschlikon Laboratory we continued our investigations of electric-field effects on the electronic structure of Cr-doped strontium titanate by means of EPR.

9.1 Studies of isotope effects in novel superconductors

9.1.1 μSR investigation of the oxygen-isotope effect on the in-plane penetration depth in cuprate high-temperature superconductors close to optimal doping

The observation of unusual oxygen-isotope (^{16}O/^{18}O) effects (OIE's) in cuprate high-temperature superconductors (HTS) on the transition temperature T_c (1; 2; 3; 4) and on the zero-temperature in-plane magnetic penetration depth $\lambda_{ab}(0)$ (3; 4; 5; 6; 7; 8; 9; 10; 11) poses a challenge to the understanding of high-temperature superconductivity. Recently, it was established that for different families of cuprate HTS there is the universal correlation between the isotope shifts of T_c and $\lambda_{ab}(0)$ (4; 7; 10; 11). Namely, in the underdoped region $\Delta T_c/T_c$ and $\Delta\lambda_{ab}(0)/\lambda_{ab}(0)$ scale linearly in respect to each other with $|\Delta T_c/T_c| \simeq |\Delta\lambda_{ab}(0)/\lambda_{ab}(0)|$. However, close to optimal doping the situation is not so clear. Khasanov *et al.* (10) observed that in optimally doped $YBa_2Cu_3O_{7-\delta}$ the small OIE on T_c is associated with a rather big isotope shift of $\lambda_{ab}(0)$ which is even compatible with that in underdoped cuprates. In contrast, Tallon *et al.* (11) found that in slightly overdoped $La_{2-x}Sr_xCu_{1-y}Zn_yO_4$ the OIE on $\lambda_{ab}(0)$ becomes zero, while the OIE on T_c remains still substantial.

In order to clarify this discrepancy the OIE's on T_c and $\lambda_{ab}(0)$ were investigated by means of magnetization and muon-spin rotation (μSR) experiments in optimally doped $YBa_2Cu_3O_{7-\delta}$ and $La_{1.85}Sr_{0.15}CuO_4$, as well as in slightly underdoped $YBa_2Cu_4O_8$ and $Y_{0.8}Pr_{0.2}Ba_2Cu_3O_{7-\delta}$. We observed a small OIE on the transition temperature T_c that is associated with a substantial OIE on the in-plane penetration depth $\lambda_{ab}(0)$ (see Fig. 9.1). The fact that a substantial oxygen-isotope effect on $\lambda_{ab}(0)$ is observed even in cuprates with a rather small OIE on T_c strongly suggests that phonons are *directly* or *indirectly* involved in the pairing. It is worth to note that in colossal magnetoresistance (CMR) manganites similar peculiar OIE on various quantities (e.g.ferromagnetic transition temperature, charge-ordering temperature) were observed (13). This suggests that in both classes of perovskites, HTS and CMR manganites, lattice vibrations play an essential role.

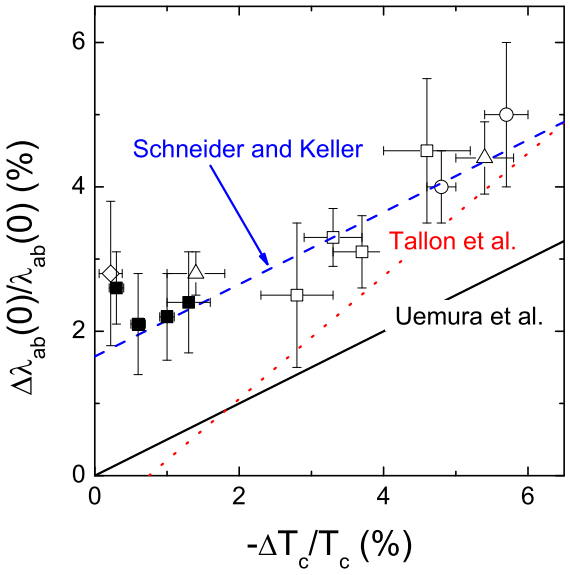

Figure 9.1: Plot of the OIE shift of the zero-temperature magnetic penetration depth $\Delta\lambda_{ab}(0)/\lambda_{ab}$(0) versus the OIE shift of the superconducting transition temperature $-\Delta T_c/T_c$ for $Y_{1-x}Pr_xBa_2Cu_3O_{7-\delta}$, $YBa_2Cu_4O_8$, and $La_{2-x}Sr_xCuO_4$ (closed squares). Open squares are bulk μSR data for $Y_{1-x}Pr_xBa_2Cu_3O_{7-\delta}$ [7; 8]. Diamonds are LE-μSR data for optimally doped $YBa_2Cu_3O_{7-\delta}$ [9]. Open circles are torque magnetization data for $La_{2-x}Sr_xCuO_4$ from [6]. Open triangles are Meissner-fraction data for$La_{2-x}Sr_xCuO_4$ [5]. The solid line corresponds to the "differential Uemura" relation with $\Delta\lambda_{ab}(0)/\lambda_{ab}(0) = 0.5|\Delta T_c/T_c|$. The dotted line corresponds to the "pseudogap" line from [11]. The dashed line indicates the flow to 2D quantum superconductor to insulator criticality as described in [12].

[1] J.P. Franck, in Physical Properties of High Temperature Superconductors IV (ed. D.M Ginsberg), 189-293 (World Scientific, Singapore, 1994).

[2] D. Zech et al., Nature **385**, 681 (1994).

[3] G.-M. Zhao, H. Keller, and K. Conder, J. Phys.: Cond. Mat. **13**, R569 (2001).

[4] H. Keller, in Structure and Bonding, Vol. 114, 143-169 (2005), A. Bussmann-Holder and K.A. Müller, eds., Springer-Verlag Berlin Heidelberg (2005).

[5] G.-M. Zhao, M.B. Hunt, H. Keller, and K.A. Müller, Nature **385**, 236 (1997).

[6] J. Hofer et al., Phys. Rev. Lett. **84**, 4192 (2000).

[7] R. Khasanov et al., J. Phys.: Condens Matter **15**, L17 (2003).

[8] R. Khasanov et al., Phys. Rev. B **68**, 220506 (2003).

[9] R. Khasanov et al., Phys. Rev. Lett. **92**, 057602 (2004).

[10] R. Khasanov et al., J. Phys.: Cond. Mat. **16**, S4439 (2004).

[11] J.L. Tallon et al., Phys. Rev. Lett. **94**, 237002 (2005).

[12] T. Schneider and H. Keller, Phys. Rev. Lett. **86**, 4899 (2001).

[13] G.M. Zhao, H. Keller, R.L. Greene, and K.A. Müller in Physics of manganites, T.A. Kaplan and S.D. Mahanti (eds.), Kluwer Academic/Plenum Publishers, New York, p. 221 (1999).

9.2 Studies of pressure effects in novel superconductors

9.2.1 Anomalous electron-phonon coupling probed on the surface of the superconductor ZrB_{12}

The traditional concept of superconductivity is strictly associated with the electron-phonon interaction. The conventional theory is based on the Migdal-Eliashberg adiabatic approximation (1) that leads to the prediction of many peculiar features which are a direct evidence of phonon-mediated superconductivity. The adiabatic approximation is valid if the parameter ω_0/E_f is small (ω_0 is the relevant phonon frequency and E_f is the Fermi energy). Most conventional superconductors satisfy this criteria with very few exceptions. Zirconium dodecaboride (ZrB_{12}) is a good candidate for anomalous (nonadiabatic) coupling. It stems from the rather small value of the Fermi energy $\sim$1 eV (2) that, together with the Debye temperature $\sim$20 meV (3), leads to a ratio ω_0/E_f $\sim$0.02. One of the key features of nonadiabatic superconductivity is the observation of unconventional isotope and pressure effects on the magnetic field penetration depth λ. Note, that in adiabatic superconductors (or in superconductors where nonadiabatic effects are small) the pressure effect (PE) (4; 5), as well as the isotope effect (IE) (6) on λ were found to be almost zero, in contrast to the substantial PE (7) and IE (8) on λ observed in highly nonadiabatic cuprate HTS.

We performed detailed studies of the PE on T_c and λ in ZrB_{12} (9). A *negative* pressure effect on T_c with $\mathrm{d}T_c/\mathrm{d}p = -0.0225(3)$ K/kbar is observed (see Fig. 9.2(a)). The magnetic field penetration depth λ measured in the Meissner state is largely determined by surface characteristics. The superfluid density $\rho_s(0) \propto \lambda^{-2}(0)$ was found to increase with pressure, with the pressure effect coefficient $\mathrm{d}\ln\lambda^{-2}(0)/\mathrm{d}p = 0.60(23)$ %/kbar (see Fig. 9.2(b)). This coefficient is much larger than that one estimated theoretically within the adiabatic approximation. This can be explained by considering that in ZrB_{12} the coupling of the charge carriers to the lattice close to the surface has a *nonadiabatic* character (9).

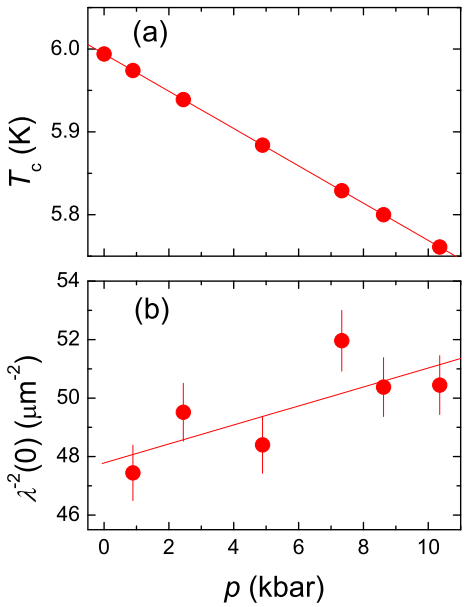

Figure 9.2: Pressure dependences of the transition temperature T_c (a) and the superfluid density $\rho_s(0) \propto \lambda^{-2}(0)$ (b) of ZrB_{12}. The solid lines are linear fits as described in [9].

[1] A.B. Migdal, Sov. Phys. JETP **7**, 996 (1958); G.M. Eliashberg, Sov. Phys. JETP **11**, 696 (1960).

[2] D. Daghero et al., Supercond. Sci. Technol. **17**, S250 (2004).

[3] R. Lortz et al., cond-mat/0502193.

[4] R. Khasanov et al., Phys. Rev. Lett. **93**, 157004 (2004).

[5] D. Di Castro et al., cond-mat/0411719.

[6] D. Di Castro et al., Phys. Rev. B **70**, 014519 (2004).

[7] R. Khasanov, J. Karpinski, and H. Keller, J. Phys.: Condens. Matter **17**, 2453 (2005).

[8] G.M. Zhao, M.B. Hunt, H. Keller, and K.A. Müller, Nature (London) **385**, 236 (1997); J. Hofer et al., Phys. Rev. Lett.

84, 4192 (2000); R. Khasanov et al., Phys. Rev. Lett. **92**, 057602 (2004); R. Khasanov et al., J. Phys.: Cond. Matt. **16**, S4439 (2004).

[9] R. Khasanov et al., Phys. Rev. B **72**, 224509 (2005).

9.2.2 Pressure effects on the superconducting properties of $YBa_2Cu_4O_8$

In the cuprate HTS the critical regime where thermal critical fluctuations dominate is experimentally accessible. It was recently shown that in this regime various critical properties are not independent, but related by universal relations (see *e.g.* (1)). Accordingly, the IE or PE on these quantities are expected to be related as well (2; 3). We performed a scaling analysis of the pressure effect on the magnetization and the in-plane penetration depth in underdoped $YBa_2Cu_4O_8$ (4). It was found that the rise of the transition temperature T_c of underdoped $YBa_2Cu_4O_8$ with increasing pressure p is associated with a decreasing anisotropy parameter γ and volume V. Figure 9.3 reveals that the relative change of the transition temperature $\Delta T_c/T_c$ is seen to mirror essentially that of the anisotropy parameter $\Delta\gamma/\gamma$. Note, that this behavior is consistent with the generic behavior for cuprate HTS, where for a given HTS family T_c increases with reduced anisotropy and thus gives a natural explanation why the PE on T_c becomes very small in optimally and overdoped cuprate HTS (5).

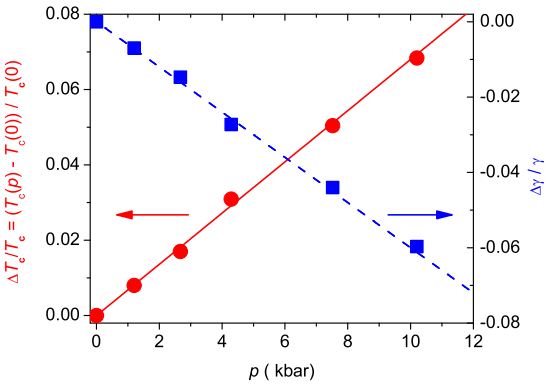

Figure 9.3: $\Delta T_c/T_c$ and $\Delta\gamma/\gamma$ versus p of $YBa_2Cu_4O_8$ obtained from the scaling analysis [4]. The solid line is $\Delta T_c/T_c = 0.0068p$ and the dashed one is $\Delta\gamma/\gamma = -0.006p$ with p in kbar.

[1] T. Schneider and J. M. Singer, *Phase Transition Approach To High Temperature Superconductivity*, (Imperial College Press, London, 2000).

[2] T. Schneider, Phys. Rev. B **67**, 134514 (2003).

[3] T. Schneider, Phys. Stat. Sol. B **242**, 58 (2005).

[4] R. Khasanov, T. Schneider, and H. Keller, Phys. Rev. B **72**, 014524 (2005).

[5] R.J. Wijngaarden, D.T. Jover, and R. Griessen, Physica B **265**, 128 (1999).

9.3 Spectroscopic studies of novel superconductors

9.3.1 EPR study of the spin-lattice relaxation of Yb^{3+}-doped $YBa_2Cu_3O_x$

The mechanism of the spin-lattice relaxation of rare-earth ions in HTS cuprates is still under debate (1; 2). Different models have been proposed to explain the experimental data. In

order to clarify this question we performed Electron Paramagnetic Resonance (EPR) measurements of Yb^{3+}-doped $YBa_2Cu_3O_x$ in a wide range of oxygen doping x (from the antiferromagnetic to the optimally doped superconducting state). The temperature dependence of the EPR line width as a function of doping x indicates that there are electronic and phononic contributions to the relaxation process. The electronic contribution increases with increasing hole doping. Figure 9.4 shows the temperature dependence of the relaxation rate for optimally doped $YBa_2Cu_3O_x$ without (T_c = 90 K) and with 3% Zn substitution (T_c = 55 K). In both samples one can see a drop of relaxation rate below T_c. This drop is more pronounced in the sample without Zn doping. However, small Zn doping cannot significantly change the phonon spectrum. Therefore, we conclude that the drop of the relaxation rate is related to a reduction of the electronic (Korringa) relaxation contribution below T_c due to the opening of the superconducting gap and a resulting decrease of the density of states at the Fermi level.

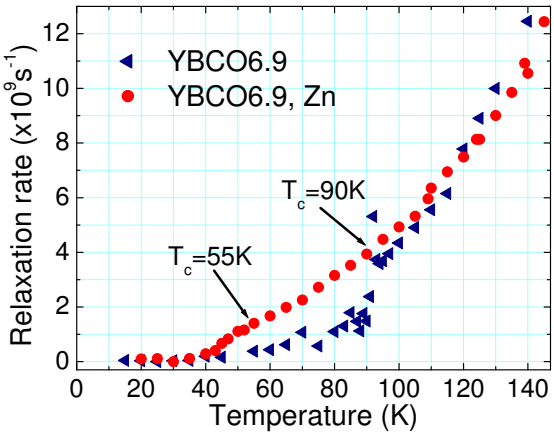

Figure 9.4: Temperature dependence of the relaxation rate for optimally doped $YBa_2Cu_3O_x$ samples with and without Zn doping.

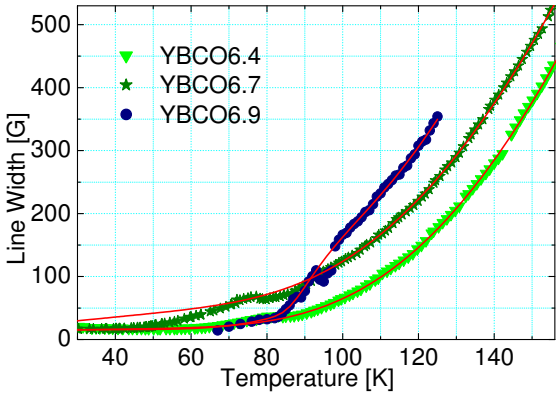

Figure 9.5: Doping dependence of the relaxation rate (line width) for $YBa_2Cu_3O_x$ ($x = 6.4, 6.7, 6.9$).

The remaining contribution to the relaxation is phononic and its temperature dependence follows an exponential function with activation energy of about 600 K. Figure 9.5 shows the temperature dependence of the relaxation rate for samples with different oxygen doping x. With decreasing x the Korringa contribution is decreasing, and for $x = 6.4$ there is practically only a phononic contribution to the relaxation.

Our results clearly show that both electronic and phononic mechanisms contribute to the relaxation of the rare-earth ions in $YBa_2Cu_3O_x$. For an optimally doped sample these contributions are approximately equal at 100 K, but at high temperatures and/or low hole-doping the phonon contribution dominates.

[1] St. W. Lovesey and U. Staub, Phys. Rev. B **64**, 066502 (2001).

[2] A. T. Boothroyd *et al.*, Phys. Rev. B **64**, 066501 (2001).

9.3.2 NMR/NQR investigations of YBCO compounds

In the search for orbital-current effects in cuprates we continued our study of various ^{89}Y NMR parameters in oriented powder samples of normal conducting $Y_2Ba_4Cu_7O_{15}$. The measurements were performed in an external magnetic field B of 9 T in the temperature range from 98 K to 300 K. Static or fluctuating magnetic fields originating from an orbital-current pattern in the CuO_2-planes as predicted (1) would appear perpendicular to the planes (parallel to the c axis) of the compound. Whereas static magnetic fields parallel to B influence the NMR linewidth only, fluctuating fields perpendicular to B alter the spin-lattice relaxation. Hence, orbital-current effects should change this ratio of investigated Y NMR parameters measured perpendicular to and parallel to the c axis, respectively. The measured ^{89}Y linewidth ratio is temperature independent within error bars. This result yields an upper limit of 0.02 mT for a possible static orbital-current field at the Y site. An estimate for the amplitude of fluctuating fields Δh_{orb} generated by the orbital-current pattern can be obtained from ^{89}Y spin-lattice relaxation measurements. The orbital-current contribution to the relaxation rate, $1/^{89}T_{1,tot}^{\perp} = 1/^{89}T_1^{\perp} + 1/^{89}T_{1,orb}^{\perp}$, changes the ratio $^{89}T_1^{||}/^{89}T_1^{\perp}$. The experimentally determined ratio, measured with two different NMR pulse schemes is temperature independent as shown in Fig. 9.6.

For the investigated temperature range, within error bars, a relative change of maximal 3% can be estimated. Provided we know the correlation time of fluctuating fields τ_c, we may estimate Δh_{orb} from this value using the relation

$$\frac{1}{^{89}T_{1,orb}^{\perp}} = \overline{\gamma^2 \Delta h_{orb}^2}^{t} \cdot \frac{\tau_c}{1+(\omega_L \tau_c)^2} < 0.03 \cdot \frac{1}{^{89}T_1^{\perp}(98K)} = 3.6 \cdot 10^{-4} s^{-1},$$

where γ denotes the gyromagnetic ratio and ω_L the Larmor frequency of ^{89}Y, respectively. τ_c may then be obtained from the underlaying energy scale of the orbital-current effect via Heisenberg's uncertainty principle. As a reasonable value the energy gap of 0.02 eV related to the pseudogap phenomena can be taken, yielding $\tau_c > 2 \cdot 10^{-13}$s. From this we obtain as an upper limit of the of fluctuating field amplitude $\Delta h_{orb} = 4.5$ mT.
A much lower energy scale has recently been observed in the plane ^{63,65}Cu spin-lattice

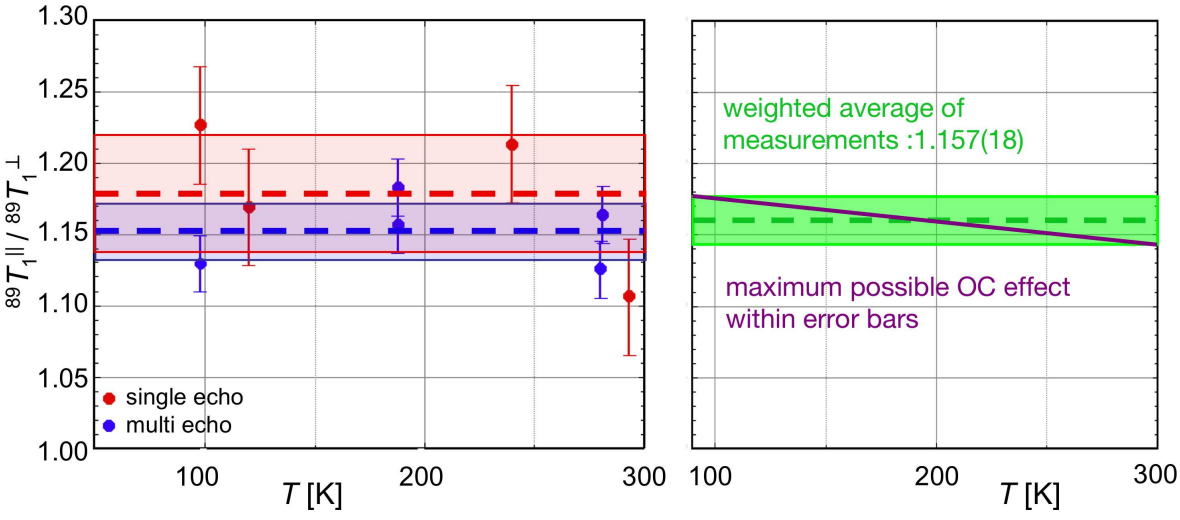

Figure 9.6: Temperature behaviour of the spin-lattice relaxation ratio $\frac{^{89}T_1^{||}}{^{89}T_1^{\perp}}$ in $Y_2Ba_4Cu_7O_{15}$ measured with two different NMR pulse schemes.

relaxation in superconducting $YBa_2Cu_4O_8$ at mK temperatures. In the superconducting phase the magnetic contribution to the Cu spin-lattice relaxation due to spin fluctuations diminishes because of the opening of the superconducting gap (2). At very low temperature this reduced relaxation progressively changes its character from magnetic towards quadrupolar (3). Moreover, it shows an unexpected rate maximum below 1 K, which can be explained by thermally activated charge fluctuations with a frequency of $\sim 10^{-10}$s and a distribution of activation energies centered at 0.09 meV ($\sim$ 1 K). This work was performed in collaboration with the research group of A.V. Dooglav and M. Eremin at the State University of Kazan and completed with ^{63,65}Cu spin-lattice measurements of the related Ca-doped compounds $Y_{1-x}Ba_{2-y}Ca_{x+y}Cu_4O_8$ (x+y = 0.02, 0.05, 0.1). During a visit of A.V. Dooglav in our group a careful reanalysis of the measurements in the Ca-doped samples was performed showing that investigations of samples with lower Ca content are necessary, in order to further clarify this exceptional behaviour of $YBa_2Cu_4O_8$ at lowest temperatures.

[1] P.A. Lee and G. Sha, Solid State Commun. **126**, 71 (2003).
[2] M. Bankay et al., Phys. Rev. B **50**, 6416 (1994).
[3] M. Mali et al., J. Supercond. **15**, 511 (2002).

9.3.3 Muon-spin rotation measurements of the penetration depth in Li_2Pd_3B

The discovery of superconductivity in the ternary boride superconductors Li_2Pd_3B and Li_2Pt_3B has attracted considerable interest in the study of these materials (1; 2; 3; 4; 5; 6). It is believed that superconductivity in both compounds is most likely mediated by phonons. It stems from photoemission (2), nuclear magnetic resonance (NMR) (3), and specific heat (6) experiments. However, experimental results concerning the structure of the superconducting energy gap are still controversal. On the one hand, NMR (3) data of Li_2Pd_3B and specific heat data of Li_2Pd_3B and Li_2Pt_3B (6) can be well explained by assuming the presence of only *one* isotropic energy gap. On the other hand, magnetic field penetration depth λ measurements suggest the presence of *two* isotropic superconducting gaps in Li_3Pd_2B and point to the presence of nodes in the gap in Li_3Pt_2B (4; 5). Systematic studies of the magnetic field and temperature dependence of λ can help to clarify this discrepancy.

Muon-spin rotation studies were performed on the ternary boride superconductor Li_2Pd_3B ($T_c \simeq 7.5$ K) (7). The following results were obtained: (i) over the whole temperature range (from T_c down to 30 mK) the temperature dependence of λ is consistent with what is expected for a single-gap s–wave BCS superconductor (Fig. 9.7), (ii) the shape of $\lambda(T)$ is almost independent of the magnetic field, (iii) at $T = 0$ the magnetic field penetration depth λ is almost field independent (inset in Fig. 9.7), as expected for a superconductor with an isotropic energy gap.

All the above mentioned features suggest that Li_2Pd_3B is *a BCS superconductor with an isotropic energy gap*.

[1] K. Togano et al., Phys. Rev. Lett. **93**, 247004 (2004).
[2] T. Yokoya et al., Phys. Rev. B **71**, 092507 (2005).
[3] M. Nishiyama et al., Phys. Rev. B **71**, 220505(R) (2005).

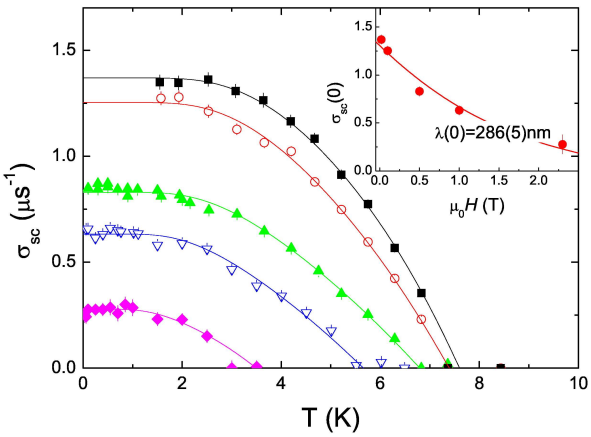

Figure 9.7:
Temperature dependence of the zero-temperature μSR depolarization rate $\sigma_{sc} \propto \lambda^{-2}$ of Li_2Pd_3B measured in various magnetic fields (from top to the bottom: 0.02 T, 0.1 T, 0.5 T, 1.0 T and 2.3 T). Solid lines represent fits with the weak-coupling BCS model [7]. The inset shows the field dependence of $\sigma_{sc}(0)$. The solid line corresponds to a fit with a field independent $\lambda(0) = 286(5)$ nm [7].

[4] H.Q. Yuan et al., cond-mat/0506771.
[5] H.Q. Yuan et al., cond-mat/0512601.
[6] H. Takeya et al., Phys. Rev. B **72**, 104506 (2005).
[7] R. Khasanov et al., cond-mat/0601156.

9.3.4 Low-energy μSR experiments in multilayers and thin superconducting films

Over recent years the μSR technique has demonstrated to be a unique and powerful microscopic tool for investigating fundamental parameters of superconductors. The low-energy μSR technique (LE-μSR) allows to explore local magnetic field profiles in HTS and/or magnetic systems near the surface of thin films and multilayer systems on a nanometer scale (1; 2). In the last year the upgrade of the LE-μSR apparatus at PSI was finished: The rate of good events approaches now 1500 per second, making the technique ready for more detailed experiments. In the first experiment with the improved apparatus a $YBa_2Cu_3O_{7-\delta}$ thin film grown at the University of Geneva was investigated. The thickness of the film was chosen to be about 200 nm which is slightly bigger than the maximum range of the low energy muons in $YBa_2Cu_3O_7$ and, on the other hand, is comparable with the magnetic field penetration depth in this material. These two circumstances made it possible to study for the first time the magnetic field profile inside a superconductor in a Meissner state when the magnetic field penetrates from both sides of a sample. The reconstructed field profile (averaged magnetic field seen by muons versus averaged muon penetration depth) is presented in Fig. 9.8.

The sample was first cooled in zero magnetic field (ZFC) from a temperature well above T_c, then a field of 195 Oe was applied parallel to the sample surface. One can see that the magnetic field penetrates (and is screened due to the supercurrent) form both surfaces of the sample achieving a minimum at the half thickness of the film, as predicted theoretically (but was never confirmed experimentally before). The solid line represents a fit with the magnetic field penetration depth $\lambda(T = 10\ \mathrm{K}) = 187(2)$ nm, which is in agreement with the literature data for nearly optimally doped $YBa_2Cu_3O_{7-\delta}$ bulk samples with T_c~87 K, confirming the good quality of the film. As a next step we are planning experiments in thin $PrBa_2Cu_3O_7$ films and $YBa_2Cu_3O_7$/ $PrBa_2Cu_3O_7$/ $YBa_2Cu_3O_7$ tri-layers with different thickness of individual layers with the goal to test a possible coupling of the superconducting $YBa_2Cu_3O_7$ layers through the antiferromagnetic $PrBa_2Cu_3O_7$ layer.

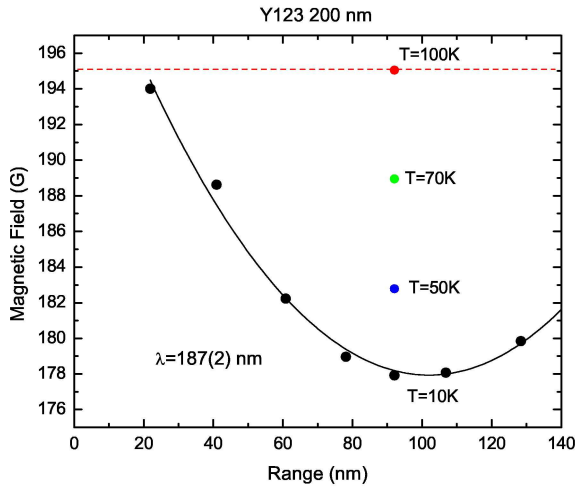

Figure 9.8: Magnetic field profile measured inside a thin (200 nm) $YBa_2Cu_3O_{7-\delta}$ film. The external magnetic field of 195 Oe is parallel to the surface of the film. One can see that the magnetic field penetrates (and is screened due to the supercurrent) from both surfaces of the sample achieving a minimum at the mid thickness of the film, as expected theoretically (but was never confirmed experimentally before). The solid line represents a fit with a magnetic field penetration depth $\lambda(T = 10\,\mathrm{K}) = 187(2)$ nm, which is in agreement with the literature data for nearly optimally doped $YBa_2Cu_3O_{7-\delta}$ bulk samples. Colored points represent a temperature scan at fixed implantation range close to the mid thickness of the sample.

[1] E. Morenzoni et al., J. Appl. Phys. **81**, 3340 (1997).
[2] T Prokscha et al., Hyperfine Interactions **159**, 227 (2004).

9.4 Electric field effects in perovskites

9.4.1 Electric field effects on Cr-doped $SrTiO_3$

In collaboration with the IBM Rüschlikon Laboratory, we are investigating resistive and switching effects that were found on thin films of perovskites like (Ba,Sr)TiO_3, $SrZrO_3$, and $SrTiO_3$ (1). These materials exhibit a charge-induced insulator-to-metal transition with a resistive memory effect. Single crystals of Cr-doped $SrTiO_3$ (2) are used as a model system for this class of materials to study the drastic resistivity changes in the bulk under applied electric field, the switching between memory levels and to clarify the role of defects with different valencies. Strontium titanate is a band insulator ($E_{gap} \approx 3.2$ eV), but when exposed to an electric field the resistance of the doped perovskite is reduced by several orders of magnitude. The conducting state is a prerequisite for the memory switching. In order to avoid the crystals to be damaged by high-power load, a typical forming procedure is performed in several steps by limiting the power (Fig. 9.9a).

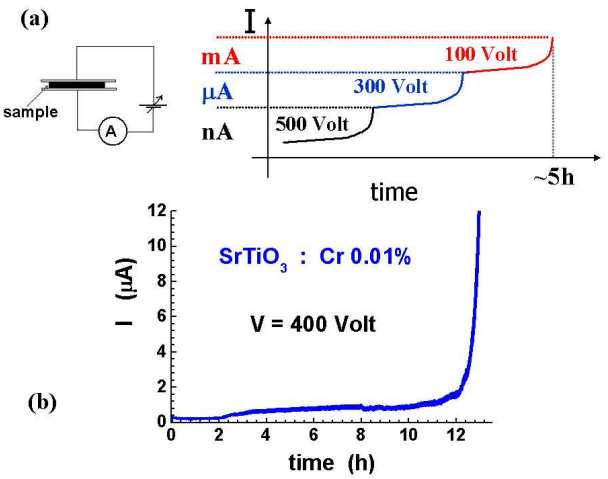

Figure 9.9: (a) Forming procedure on a Cr-doped $SrTiO_3$ single crystal. Once the current reaches the compliance the voltage source is decreased in order to avoid power damage. (b) The increase of the conductivity shows a drastical change after long-time exposure to high voltage.

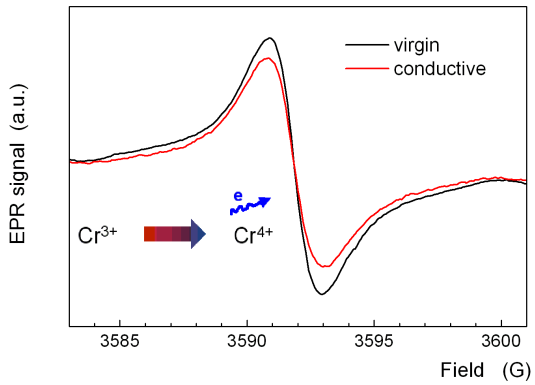

Figure 9.10:
Comparison of the EPR signal of Cr^{3+} in Cr-doped $SrTiO_3$ between a virgin and a conductive sample.

We prepared a series of single crystals to systematically investigate the effects in a wide range of the Cr doping (from 0.001 to 0.2 molar %). A decreasing forming time by increasing the Cr content was observed. Figure 9.9b shows the typical behavior of one forming step in a sample with 0.01 molar % of Cr. Here the conductivity increases by one order of magnitude in 12h. At the higher amount of Cr (0.2 molar %) the full forming procedure takes only a day. Another clear evidence of the Cr influence on the forming procedure is reported in Ref. (4) where changes of the electronic state of the Cr dopant are detected by X-ray absorption spectroscopy on crystals. During electrical stressing they observed the transformation of Cr^{3+} to Cr^{4+} in a volume close to the metal electrode (anode). Because the X-ray absorption collects information restricted to the surface region, we decided to study these materials using electron paramagnetic resonance (EPR) which allows to distinguish different valence states of Cr and probes the entire bulk. In Fig. 9.10 we compare the EPR signal of Cr^{3+} at room temperature in the insulating and the conducting state. The amount of Cr^{3+} decreases in the conductive state.

The simplest process we assume to explain the decreasing of the Cr^{3+} EPR signal is a ionization of the Cr site which increases its valence by one unit (Fig. 9.10). The nature of the free carriers in the conductive state and their precursor centers are still open questions. In order to clarify the role of the electron removed from the Cr site, it is important to understand whether there is a correlation between the conductivity and the amount Cr^{3+} centers. Therefore, a special sample holder will be developed for in-situ experiments which will allow to apply an electric field to the $SrTiO_3$ crystals directly in the resonance cavity. This will allow the study of changes in the electronic state of Cr during the electrical stressing, leading to the insulator-to-metal transition at the different conductive states and possibly will help to clarify its microscopic mechanism.

[1] A. Beck et al., Appl. Phys. Lett. **77**, 139 (2000).
[2] Y. Watanabe et al., Appl. Phys. Lett. **78**, 3738 (2001).
[3] K.A. Müller et al., Solid State Commun. **85**, 381 (1993).
[4] I. Meijer et al., Phys. Rev. B **72**, 155102 (2005).

9.5 New developments in instrumentation

9.5.1 Soft- and hardware upgrade of the 5.5T-MPMS

Due to the ongoing interest in investigating magnetic properties of novel materials in our laboratory we decided to update our 5.5T-MPMS (Magnetic Properties Measurement System) to a more modern measurement platform. The company *Quantum Design* offered us an installation procedure which allows an update to a *Windows* based software called *MultiVu*. This is not simply done by installing the corresponding program files, also the CPU of the MPMS control board, the EPROM drive, and the measuring PC needed to be replaced. This was achieved by using a faster *Pentium* Computer running under *Windows XP*. We have chosen *Windows XP* as operating system, because it is more robust than the earlier *Windows* versions and allows a convenient way to handle GPIB-interfaces. The installation has worked out without any significant problems. A recalibration of the system was not needed; the relevant values and factors for the field calculation and the measurement algorithms were simply copied from the older software. We checked many of the calibration factors after the update by some simple test measurements on $La_{1.85}Sr_{0.15}CuO_4$ single crystals in order to make sure that the system works properly. With the help of the new and much more helpful diagnostics menu of *MultiVu* we now have access to more system parameters during a measurement and we can check any anomaly during a programmed sequence without aborting the current run.

9.5.2 NMR insert device for the 9T-PPMS

A 9T-PPMS (Physical Properties Measurement System) is a very flexible equipment for various types of measurements to be performed at temperatures from 1.8 K to 300 K and in any field from 0 T to 9 T. These features make it very attractive to extend the range of our NMR equipment to temperatures below liquid helium and to use swept field procedures for broad line NMR studies. In the framework of a diploma thesis (1) performed in the research group of Prof. A. Schilling a NMR insert adapted to the specifications of the PPMS was constructed and a new software was designed in order to run the PPMS fully under control of the NMR system. Extensive tests showed that the new NMR-PPMS apparatus is fully operational.

[1] Alexander Gafner, Diploma thesis, Physik-Institut, Universität Zürich (2006).